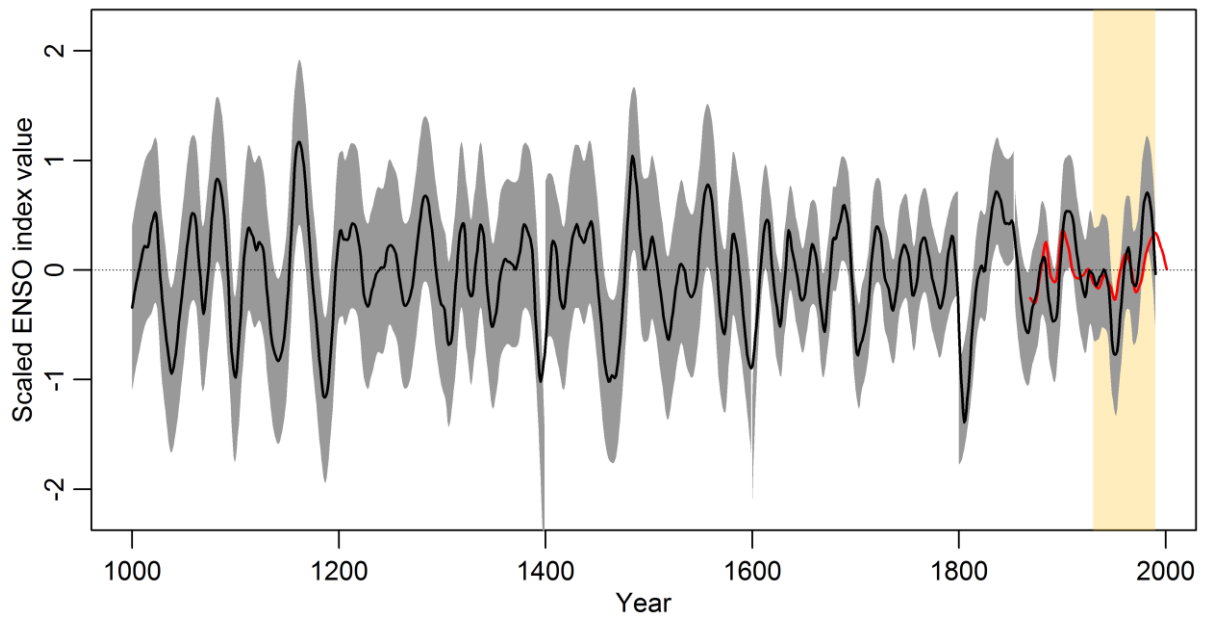


## S1 ENSO DJF Reconstruction



**Figure S1** 31-year filtered ENSO index reconstruction. The target ENSO index is shown in red. The shading indicates its 95% confidence range and the orange shading corresponds to the reference period 1930-1990

## **S2 Proxy Data: Overlaps and climate variable allocation**

### **S2.1 Data overlaps in ENSO and SAM reconstructions**

Since both the SAM and ENSO reconstructions share some of the initial proxy record data bases, there are some proxy records contributing to both reconstructions. However, there are only three overlapping proxy records. Hence, this overlap is very small (3 out of 64 in the case of the ENSO reconstructions and 3 out of 34 in case of the SAM reconstruction). The records in question are a coral record (Fiji  $\delta^{18}\text{O}$ , ID 36), a documentary record (from the area de Trujillo, ID85) and an ice core record (Law Dome summer sea salt, ID 441). Our reconstruction methods take out the part of the variability in the proxy records that matches with the target index. Hence we conclude that this minor overlap does not affect the validity of our results when the two reconstructions are compared.

### **S2.2 Allocation of records to climatic variables for pseudoproxy generation**

As described in the main text, noisy pseudo-proxies from tree and coral archives are generated using proxy system models. To generate the noise-based pseudo-proxies from other archives and the perfect pseudoproxies, each record is assigned to a climatic variable: coral records are all assigned to temperature. Documentary records are all specific temperature or rainfall proxies and are therefore allocated to the respective variable. Ice core accumulation records are allocated to precipitation, whereas ice core isotope records are allocated to temperature. Tree-ring records usually reflect a mixed signal. Hence, the variable is identified by correlating model temperature and precipitation at the proxy location with the target (ENSO or SAM) index and selecting the variable with the higher correlation. The same procedure was applied to ice core chemical data, where the climate relationship is often not clear. Two records were allocated to a variable based on the literature: Illimani  $\text{NH}_4$  ice core record: temperature, Lake Challa warve thickness: precipitation. We note that this process reflects a simplification of the true climate signal, but we argue this is defensible given the number of non-tree and coral records is comparatively small. Also note that the performance of perfect pseudo-proxies is lower than expected in the CESM model because the correlation of local climate to large-scale averages is weaker than in the real-world (Neukom et al., 2018). Fig. 3 shows that the perfect pseudoproxies do not yield higher reconstruction skill than the real-proxy reconstructions, showing that our correlation-based identification of the “optimal” climate variable for each proxy does not generate pseudo-proxies with unrealistically high proxy-climate relationships in the context of our index reconstructions.

### S3 Superposed Epoch Analyses

Figure S2 shows the SEA with 31-year running correlations between ENSO and SAM reconstructions which does not yield a significant response in the years following major volcanic eruptions.

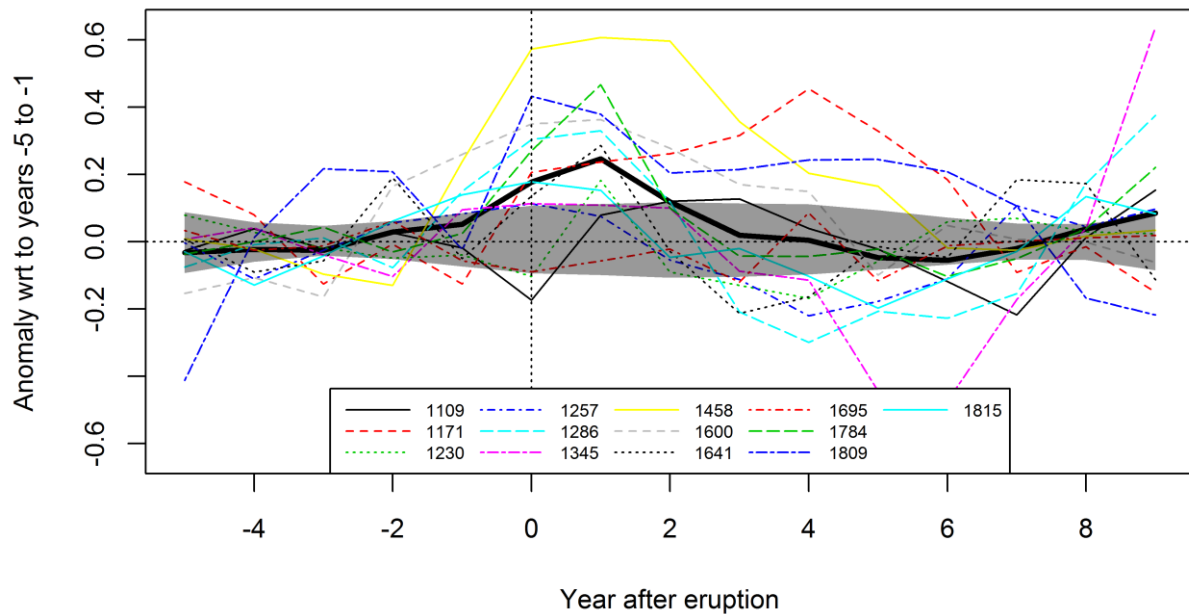


**Figure S2** SEA with 31-year running correlations between ENSO and SAM reconstructions. Threshold for eruptions: 0.15

The SEA with 31-year running correlations between the 13 model ENSO and SAM indices does not yield consistent results. In 8 cases there is no significant response. The results for the 5 cases showing a significant response is as follows:

- positive response at year 7
- negative response at years 2, 3 and 4
- positive response at year 7 and a negative response at year 8
- positive response at years 2, 4 and 5 and a negative response at year 8
- positive response at year 2

### S4 Running correlations between Model ENSO and SAM

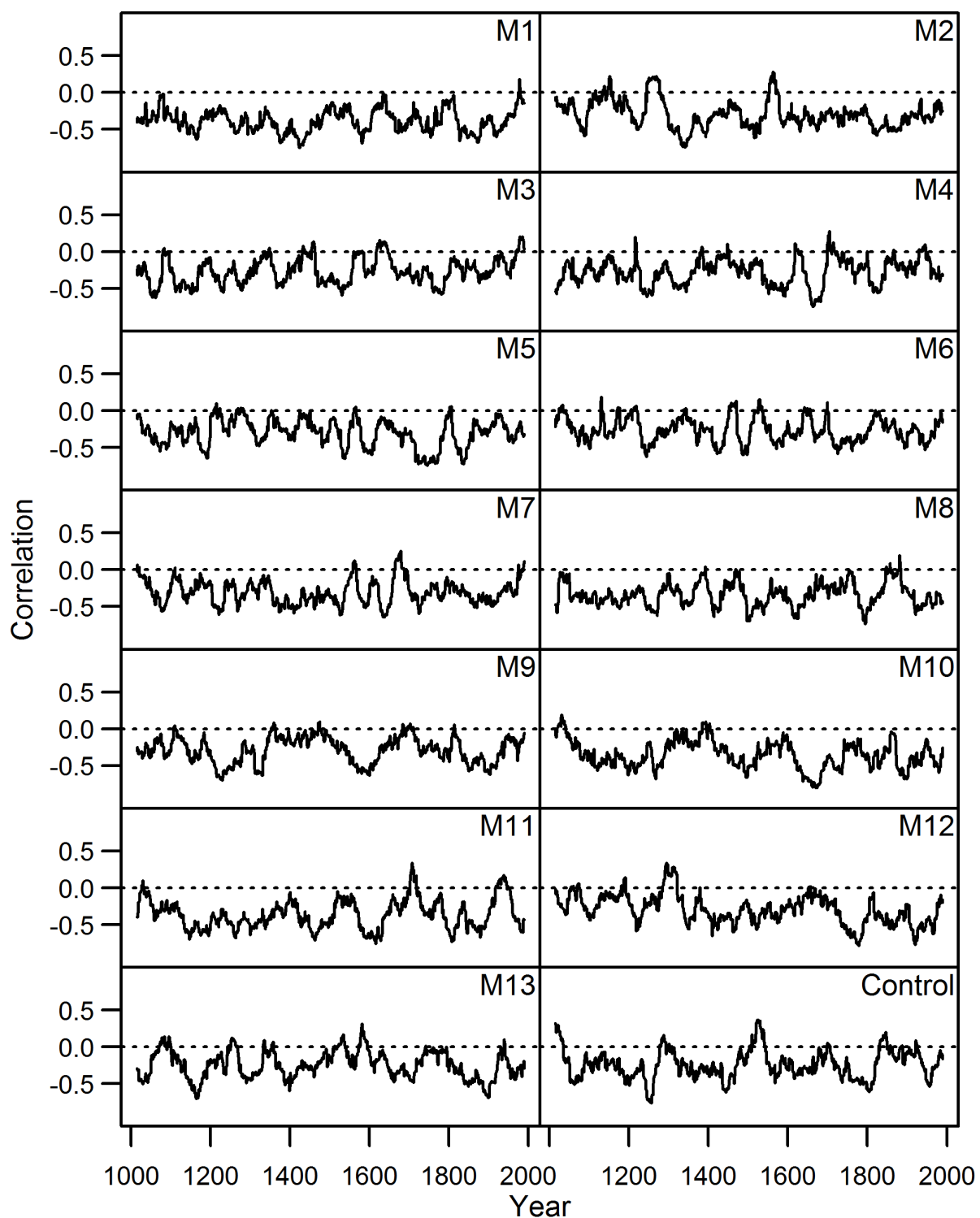


**Figure S3** Running correlations between ENSO and SAM indices for all 13 CESM model runs (M1-M13) plus the control run (Control)

## S5 Spatial temperature and SLP patterns in the model world during periods of positive and very strong negative teleconnections using alternative parameters

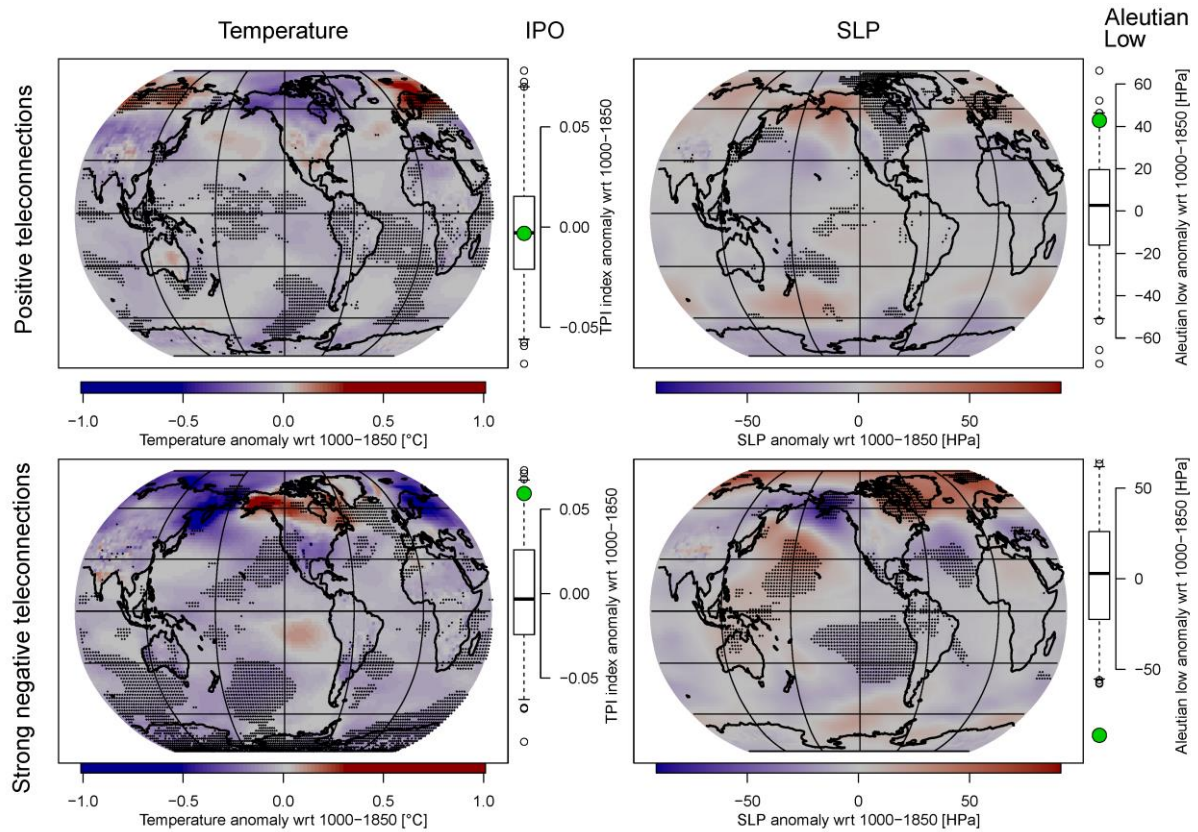


**Figure S4** Same as Fig. 4 but using a different threshold for reversed teleconnections: two instead of three standard deviations above the mean, yielding a threshold correlation of  $+0.07$ , which is exceeded during 434 years in all available years from 13 transient simulations plus the control run

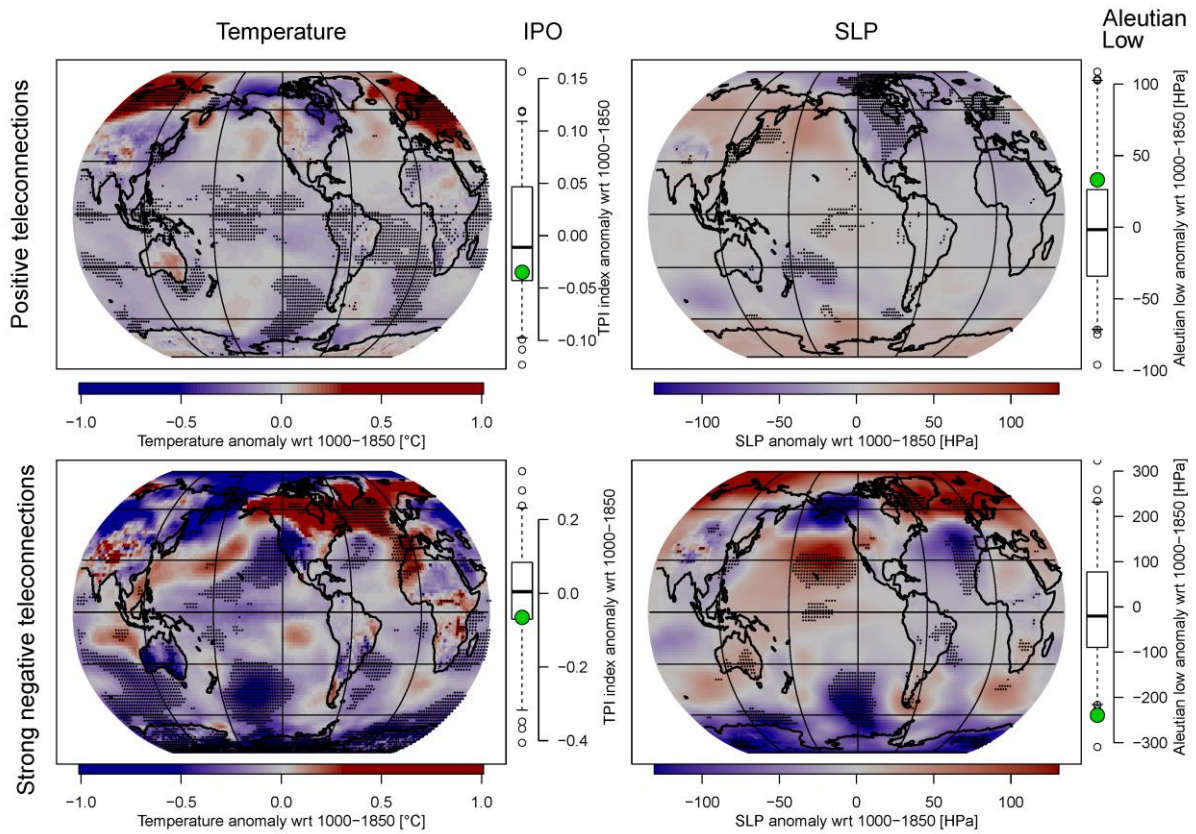


**Figure S5** Same as Fig. 4 but using a threshold of 2.5 standard deviations above the mean for both positive and negative correlations leading to 168 and 22 years selected for reverse and strong teleconnections, respectively

## References

Neukom, R., Schurer, A. P., Steiger, N. J., and Hegerl, G. C.: Possible causes of data model discrepancy in the temperature history of the last Millennium, *Sci. Rep.*, 8, 7572, doi:10.1038/s41598-018-25862-2, 2018.